

# Mobile Target Detection in Wireless Sensor Networks With Adjustable Sensing Frequency

Yanling Hu, Mianxiong Dong, *Member, IEEE*, Kaoru Ota, *Member, IEEE*, Anfeng Liu, and Minyi Guo, *Senior Member, IEEE*

**Abstract**—How to sense and monitor the environment with high quality is an important research subject in the Internet of Things (IOT). This paper deals with the important issue of the balance between the quality of target detection and lifetime in wireless sensor networks. Two target-monitoring schemes are proposed. One scheme is Target Detection with Sensing Frequency  $K$  (TDSFK), which distributes the sensing time that currently is only on a portion of the sensing period into the entire sensing period. That is, the sensing frequency increases from 1 to  $K$ . The other scheme is Target Detection with Adjustable Sensing Frequency (TDASF), which adjusts the sensing frequency on those nodes that have residual energy. The simulation results show that the TDASF scheme can improve the network lifetime by more than 17.4% and can reduce the weighted detection delay by more than 101.6%.

**Index Terms**—Delay, moving target detection, network lifetime, sensing frequency, wireless sensor networks (WSNs).

## I. INTRODUCTION

INTERNET of Things (IOT) is a worldwide network of interconnected objects based on standard communication protocols, and it is commonly accepted as the next generation of Internet [1]. A wireless sensor network (WSN) is composed of a large number of cheap sensor nodes that deployed in the monitoring area and communicate with each other to sense and measure the surrounding environment. A WSN is an important form of the underlying network technology of IOT. An important application in WSNs is to sense and monitor the moving target intelligently.

Although there have been many studies on target detection, most of them focus on how to optimize the duty cycle of nodes

to optimize the target detection quality [2]–[7]. The quality of target detection mainly includes the delay for detection, the probability of missing a target, and the network lifetime. Wu *et al.* [5] pointed out that, in WSNs, a node wakes up periodically to detect the target and to receive or send data to the sink or the next-hop node. After that, it will reenter the sleep mode. Therefore, a nodal cycle consists of wake and sleep states. Generally speaking, the duty cycle of nodes should be relatively small in order to save energy. Thus, the nodes will go through a short wake time after the long sleep state. When a node is in sleep, the target will not be detected, which leads to a blind period in the detection. The sensing frequency of this scheme is 1 in a perceived cycle. We call it the Target Detection with Sensing Frequency One (TDSFO) scheme. To improve the target-monitoring quality, a new intelligent solution called the Target Detection with Sensing Frequency  $K$  (TDSFK) scheme is proposed. The main idea of the TDSFK is to divide the sensing duty cycle into small pieces within the wake state of nodes, so that there is no long sleep state for nodes. The quality of target detection is thus enhanced. However, the TDSFK scheme has to pay the energy consumption for the state transition, which is given less consideration by the previous studies. The authors in [5] noticed that the processors and sensors for the state transition need certain energy. They also pointed out that the Mica mote sensor requires 4 ms to start [5]. Hence, how to optimize the given sensing frequency of node to increase the lifetime and improve the monitoring quality is an important research issue. We also propose a method called the Target Detection with Adjustable Sensing Frequency (TDASF) scheme, which is based on adopting different sensing frequency in distinct regions of the network. The TDASF scheme can further improve the quality of target detection. The main contributions in this paper are presented as follows:

- 1) We first analyze the relationship between the sensing frequency of nodes and sensing quality of the network and the relationship between the energy consumption of a node and its sensing frequency. Then, a tradeoff optimization scheme between detecting quality and network lifetime is given.
- 2) Based on the aforementioned optimization, an optimized method of unequal sensing frequency is put forward, which can improve the monitoring quality of the network greatly. A novel measurement framework called the Weighted Quality of Target Detection (WQTD) is also proposed for evaluating the quality of target detection. Nodes from area to area have different duty cycles; hence,

Manuscript received September 9, 2013; revised December 26, 2013; accepted February 2, 2014. Date of publication June 24, 2014; date of current version August 23, 2016. This work was supported in part by the National Natural Science Foundation of China under Grant 61379110, Grant 61073104, Grant 61073186, Grant 61272494, and Grant 61309027; the National Basic Research Program of China (973 Program) under Grant 2014CB046305; the Open Research Project of the State Key Laboratory of Industrial Control Technology, Zhejiang University, China (No. ICT1407), JSPS KAKENHI Grant Number 25880002, 26730056 and JSPS A3 Foresight Program. (*Corresponding author: A. Liu.*)

Y. Hu and A. Liu are with the School of Information Science and Engineering, Central South University, Changsha, 410083 China (e-mail: afengliu@mail.csu.edu.cn).

M. Dong is with the National Institute of Information and Communications Technology (NICT), Tokyo 184-8795, Japan.

K. Ota is with the Department of Information and Electronic Engineering, Muroran Institute of Technology, Muroran 050-8585, Japan.

M. Guo is with the Department of Computer Science and Engineering, Shanghai Jiao Tong University, Shanghai 200030, China.

Digital Object Identifier 10.1109/JSYST.2014.2308391

the quality of the target detection is also different with their distances to the sink. In this paper, we measure the overall quality of target detection by the weighting method. As the WQTD considered the uneven nature of the system, it can be effectively used to evaluate the quality of target detection and the performance of the detection scheme.

- 3) Through our extensive theoretical analysis and simulation study, we demonstrate that, for such systems, both target detection performance and energy efficiency can be achieved simultaneously. We also demonstrate that our scheme has significantly improved from both a single quality indicator and the overall performance indicators. This is difficult to be achieved in the past study.

The rest of this paper is organized as follows: In Section II, the related works are reviewed. The system model is described in Section III. In Section IV, a novel TDA SF scheme is presented. Performance analysis is provided in Section V. Section VI presents the experimental results and comparison. We conclude in Section VII.

## II. RELATED WORK

There have been many studies on target detection. Huang *et al.* [8] studied the optimal placement of sensors with the goal of minimizing the number of installed devices, while ensuring coverage of target points, and wireless connectivity among sensors. There were some researchers who took a different approach by choosing proper nodes from the deployed network to compose coverage and connectivity to play a monitoring role [9]. Liu and Towsley [10] evaluated coverage quality when sensors are distributed according to a 2-D Poisson point process. Different from the previous research, Rout and Ghosh [11] introduced and studied the problem of designing WSNS for the detection of mobile targets traversing a sensitive region along specific paths.

On one hand, the sensing range of sensor nodes has to cover the monitoring area. On the other hand, because the energy of sensor nodes is very limited, if a node has been always in the active state, the energy consumption of the node is considerably high, although the targets within the scope of coverage can be detected. Hence, the method used by most studies on target detection makes the nodes work and sleep periodically to save energy. Due to the fact that the sensor nodes often have redundancy when deployed, the monitoring quality still can be achieved at a higher standard even if the duty cycle is small, and the network lifetime will be greatly prolonged. Therefore, most researchers focus on how to optimize the duty cycle of nodes (nodes' wake-up strategies) to optimize the target detection quality [2]–[7], [11]–[13]. The sensor node consists of sensing and communication devices. The sensing device is for target detection, and the communication device is used for data communication. The total energy of the node is certain, and there is a tradeoff optimization relation between the energy consumption used for detection and for communication: if we assign more energy to the sensing device, the monitoring quality is high. On the contrary, if we assign more energy to the communication device, the internal nodes are at the working

state with high probability when the external nodes have data to be transmitted in the route. Then, the delay for data getting to the sink will be less. Based on the previous analysis, the main design goal in [2] and [7] is to maximize the operational lifetime of the system, while ensuring high target detection performance and short response time. They put forward a cross-layer optimization method between sensing (for detection) and communication layers.

There are many optimization algorithms. However, the duty cycle of nodes is often in connection with the network load. Therefore, we need a method with adaptive duty cycles that can meet the monitoring quality when adopting the minimum duty cycle, to maximize the network lifetime. Based on the aforementioned ideas, Byun and Yu [14] and Ota *et al.* [15] proposed a control-based approach for the duty cycle adaptation through the queue management to achieve high performance under variable traffic rates for WSNS. To have energy efficiency while minimizing the delay, they design a feedback controller, which adapts the sleep time to the traffic change dynamically by constraining the queue length at a predetermined value.

In conclusion, the current research has two shortcomings: 1) the entire network adopts the same node duty cycle. This results in the unbalance of energy consumption. The residual energy of nonhotspot nodes in the network will be wasted. 2) The nodes in the active state were arranged in a continuous period of time. It leads to a longer perceived gap and then affects the monitoring quality. In this paper, we propose the two target-monitoring schemes TDSFK and TDA SF to intelligently adjust the sensing frequency, thus overcome these two shortcomings.

## III. SYSTEM MODEL AND PROBLEM STATEMENT

### A. Network Model

Our network model is similar to the model used in [2] and [7]. In this network, a large number of acoustic sensors are deployed with density  $\rho$  to monitor the activities and locations of the animals in a natural habitat continuously [16]–[18]. As soon as the trends of endangered species (incoming targets) are detected, the corresponding source nodes nearby will report data periodically to the sink node [19]. WSNS can also keep monitoring when the hunter enters the protected area. Once the hunter appears, an alert message will be sent to the sink. In this way, the message sent for the control center outside the network protects the endangered species from hunters [20].

The network radius is  $R$ . All the targets are randomly distributed in the network. Hence, the probabilities of the targets monitored by each sensor node are equal. Likewise, the probabilities of generating data are equal as well.

### B. Problem Statement

Mobile target detection is a problem of multiple-target optimization. The goal here is to maximize the network lifetime and, at the same time, to minimize the probability of missing a target. Similar to that in [2] and [7], the target detection of a WSN can be characterized by several performance indicators, as explained in the following.

- 1) Delay for detection (denoted by  $D_{\text{det}}$ ).  $D_{\text{det}}$  refers to the time from the ingoing moment of the target to being detected by any sensor for the first time.
- 2) The probability of missing a single incoming target (denoted by  $P_{\text{md}}$ ).  $P_{\text{md}}$  refers to the probability of not being detected by any sensor node, when the target goes through the monitoring area.
- 3) The probabilities of missing all incoming targets (denoted by  $P_{\text{ma}}$ ).  $P_{\text{ma}}$  refers to the probability of all the targets not being detected by the node when passing through the monitoring area.
- 4) The probabilities of missing at least one of the incoming targets (denoted by  $P_{\text{mo}}$ ).  $P_{\text{mo}}$  refers to the probability of at least one target not being detected by the sensor node, when multiple targets go through the monitoring area.
- 5) Lifetime (denoted by  $\ell$ ). Similar to the definition in [21], lifetime is defined as the death time of the first node in the network.

Obviously, the goal of target detection can be stated as follows:

$$\begin{cases} \min(D_{\text{det}}, \min(P_{\text{md}})) \\ \min(P_{\text{ma}}, \min(P_{\text{mo}}), \max(\ell)) \\ \text{s.t. } D_{\text{det}} \leq D_{\text{det}}^{\ominus}, P_{\text{md}} \leq P_{\text{md}}^{\ominus} \\ P_{\text{ma}} \leq P_{\text{ma}}^{\ominus}, P_{\text{mo}} \leq P_{\text{mo}}^{\ominus}. \end{cases} \quad (1)$$

In (1),  $D_{\text{det}}^{\ominus}$ ,  $P_{\text{md}}^{\ominus}$ ,  $P_{\text{ma}}^{\ominus}$ , and  $P_{\text{mo}}^{\ominus}$  represent the minimum requirements of monitoring performance thresholds  $D_{\text{det}}$ ,  $P_{\text{md}}$ ,  $P_{\text{ma}}$ , and  $P_{\text{mo}}$  in applications. The goal of (1) is to minimize the monitoring performances  $D_{\text{det}}$ ,  $P_{\text{md}}$ ,  $P_{\text{ma}}$ , and  $P_{\text{mo}}$  and to keep them not less than the minimum requirements of the application performance. Meanwhile, maximize the lifetime as much as possible.

In the previous studies [2], the authors assume that all sensor nodes have the same values of network parameters and sensing frequency. This strategy is referred to as Target Detection with Same Sensing Frequency (TDSSF) in this paper. Therefore, the monitoring performances of nodes are equal everywhere in the network. As indicated before, if using the same monitoring parameters, the nonhotspot area will have a lot of residual energy. In this paper, the nonhotspot nodes are set with greater sensing frequency for higher monitoring performance. Thus, the target detection performance of different regions of the network will be unequal. In order to evaluate the uneven monitoring performance better, a novel measurement framework WQTD is proposed. The monitoring performance of WQTD is represented as follows:

$$f_i^w = \sum_{j \in \Omega} \left( f_i^j \cdot \frac{n_j}{n} \right). \quad (2)$$

In (2),  $f_i^w$  represents the performance indicators of node  $i$  after weighted (refers to  $D_{\text{det}}$ ,  $P_{\text{md}}$ ,  $P_{\text{ma}}$ , and  $P_{\text{mo}}$ ). Lifetime  $\ell$  is not included because it means the death time of the first node.  $f_i^j$  represents that the performance index order of the  $i$ th node is  $j$ .  $n$  is the total number of nodes in the network.  $n_j$  is the number of indicator in  $j$  indicators.

In the scheme of TDASF, increasing the sensing frequency of the nonhotspot nodes uses their remaining energy. The mon-

itoring performances are different from area to area because the energy is often not equal. Let the delay for detection be  $D_{\text{det}}^x$  for nodes at  $x$  meters away from the sink. The delay in the entire network is given by

$$D_{\text{det}}^w = \int_0^R \int_0^{2\pi} D_{\text{det}}^x \cdot x \cdot dx \cdot d\theta. \quad (3)$$

Similarly, other weighted monitoring performance indicators can be given as follows:  $P_{\text{md}}^w$ ,  $P_{\text{ma}}^w$ , and  $P_{\text{mo}}^w$ .

The network lifetime  $\ell$  depends on the node that spends the most energy. The energy consumption of node  $i$  consists of 1) communication energy. For instance,  $e_i^t$  and  $e_i^r$  are used for transmitting and receiving data; 2) sensing energy consumption  $e_i^{\text{sen}}$ ; 3) the consumption in the Low-Power-Listening (LPL) state, i.e.,  $e_i^{\text{LPL}}$ ; and (d) the consumption in the sleep state, i.e.,  $e_i^s$ . Because the death time of the first node is defined as lifetime, minimizing the energy consumption of the node that spends the most can be expressed as the following formula:

$$\max(\ell) = \min \max_{0 < i \leq n} (e_i^t + e_i^r + e_i^{\text{sen}} + e_i^{\text{LPL}} + e_i^s). \quad (4)$$

In conclusion, the design of TDASF is prolonging the system lifetime to meet application requirements. The goal of TDASF proposed in this paper can be obtained as

$$\begin{cases} \min(D_{\text{det}}^w, \min(P_{\text{md}}^w), \min(P_{\text{ma}}^w), \min(P_{\text{mo}}^w)) \\ \max(\ell) = \min \max_{0 < i \leq n} (e_i^t + e_i^r + e_i^{\text{sen}} + e_i^{\text{LPL}} + e_i^s) \\ \text{s.t. } \max(D_{\text{det}}^x) \leq D_{\text{det}}^{\ominus} \\ \max(P_{\text{md}}^x) \leq P_{\text{md}}^{\ominus}, \max(P_{\text{ma}}^x) \leq P_{\text{ma}}^{\ominus}, \max(P_{\text{mo}}^x) \leq P_{\text{mo}}^{\ominus}. \end{cases} \quad (5)$$

Equation (5) is the same as (4) for lifetime  $\ell$ . As for other monitoring performances, it means to optimize the weighted performances and make the maximum performance indicators meet the required thresholds of application.

### C. WSN Model

A sensor node is composed of two major units: a sensing device and a communication subunit. Ideally, each unit can have separate power control [2]. The communication subunit does not necessarily have the same duty cycle with the sensing device [21]. In order to reduce the energy consumption of the system, the sensing part and the communication subunit can be periodically switched off, according to a normalized duty cycle. The duty cycle of the sensor node is defined as its active/working period. Every unit has its own duty cycle since the two major units control their status independently.

For the sensing device, its duty cycle called sensing duty cycle is denoted by  $\varsigma_{\text{sen}}$  in (6), and the other called communication duty cycle is denoted by  $\varsigma_{\text{com}}$  in (7), as follows:

$$\varsigma_{\text{sen}} = t_{\text{sen}}^a / t_{\text{sen}} = t_{\text{sen}}^a / (t_{\text{sen}}^a + t_{\text{sen}}^{\text{off}} + t_c) \quad (6)$$

where  $t_{\text{sen}}$  is the time length of a unit sensing cycle, and  $t_{\text{sen}}^a$  is the valid sensing time by the sensing device. While  $t_{\text{sen}}^{\text{off}}$  is the time that the sensing device lasts when it is off in a cycle.  $t_c$

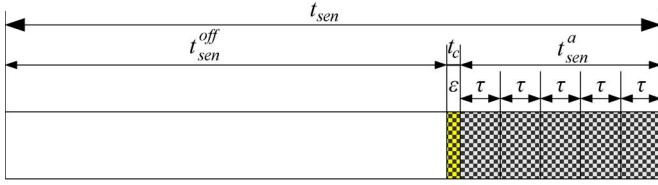


Fig. 1. TDSFO scheme (sensing frequency is 1).

 TABLE I  
 MAIN NOTATIONS AND VALUES ADOPTED IN THIS PAPER

| Symbol           | Description   | Value                  |
|------------------|---|------------------------|
| $t_{com}$        | Communication period of duration                                    | 250ms                  |
| $t_{sen}$        | Sensing period of duration  | 15s                    |
| $r_s$            | Perceived radius  | 20m                    |
| $\epsilon_c$     | Conversion power consumption  | 0.005W                 |
| $\epsilon_{sen}$ | Sensing power consumption   | 0.0036W                |
| $\omega_R$       | The power used by a node to receive a packet;                       | Calculation-specific   |
| $\omega_T$       | The power used to transmit an alert packet                          | Calculation-specific   |
| $\epsilon_t$     | Transmission power consumption                                      | 0.0511W                |
| $\epsilon_r$     | Reception power consumption   | 0.0588W                |
| $\epsilon_s$     | Sleep power consumption   | $2.4 \times 10^{-7}$ W |
| $P_d$            | The target detection probability                                    | 0.1                    |
| $N_{tar}$        | The number of times that a target appears during a reference period | 10                     |
| $\omega_s$       | The power when node is in sleep                                     | Calculation-specific   |
| $S_p$            | Preamble duration   | 0.26ms                 |
| $S_{al}$         | Ack window duration   | 0.26ms                 |
| $S_d$            | Packet duration   | 0.93ms                 |
| $\epsilon_s$     | Sleep power consumption   | $2.4 \times 10^{-7}$ W |

is the time for the transition from the sleep state to the sensing state (in Fig. 1,  $t_c = \epsilon$ ). That is

$$\zeta_{com} = t_{com}^a / t_{com} = t_{com}^a / (t_{com}^a + t_{com}^{off}) \quad (7)$$

where  $t_{com}$  is a communication cycle time,  $t_{com}^a$  is the duration when the communication subunit is active, and  $t_{com}^{off}$  is the time length when the communication subunit is in sleep. The duty cycle starts over between two consecutive periods.

The main notations and values adopted in this paper are concluded in Table I.

#### IV. DESIGN OF TDSFK SCHEME

##### A. Proposal of TDSFK Scheme

In the previous studies [7], researchers divided the sensing cycle of a node into two states: one is the sensing state, and the other is the sleep state. The change from the sleep state to the sensing state lasts for  $\epsilon$  (i.e.,  $t_c$ ), and the energy consumption

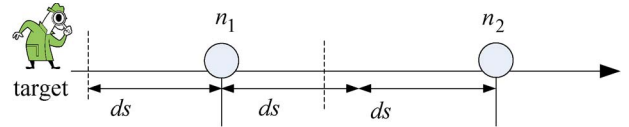


Fig. 2. Schematic diagram of target detection in a linear network.

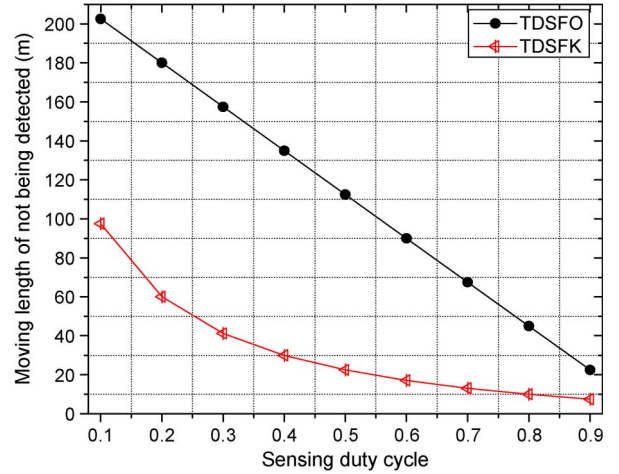


Fig. 3. Moving distances in different sensing duty cycles.

for state transition is  $\epsilon_c$ . The minimum time slot for a node to sense once is  $\tau$ . If the node in the sensing state is composed of  $k$  minimum time slots, then  $t_{sen}^a = k\tau | k \geq 1$ . In such a strategy, a duty cycle is composed of a continuous sleep time ( $t_{sen}^{off}$ ), the transition time from sleep to sensing state ( $t_c$ ), and a continuous sensing time ( $t_{sen}^a$ ), as shown in Fig. 1. In this strategy, a duty cycle has only one continuous sensing period, i.e., the sensing frequency is 1. It is called the TDSFO scheme.

In TDSFO, if a node is in the sleep state for a long period of time  $t_{sen}^{off}$  and cannot detect the target, it may miss the target. Here, we illustrate the performance of TDSFO scheme by a simple example. Suppose that, in a linear network such as that shown in Fig. 2, the target accesses the network from the left and tries to pass through the network. The movement speed of target is  $v$  (m/s). The sensing cycle time of node is  $T$  (s), and the sensing duty cycle is  $\zeta_{sen}$  (%). Suppose that the target is intelligent and able to enter the network just when the first node ( $n_1$ ) begins to change over to the sleep state. Then, when the target passes by a node ( $n_1$ ), it is able to move for a distance  $L_1 = vT(1 - \zeta_{sen})$  without being detected. If  $L_1 < 2ds$  (the monitoring range of  $n_1$ ), the overall moving distance of not being detected is  $L_1$ . On the contrary, if  $L_1 > 2ds$ , the target can move to  $n_2$ 's monitoring range. The target can still be undetected and move some distance in a certain probability. Fig. 3 is given when  $v = 15$  m/s,  $T = 15$  s, the distance that the target is able to move when  $\zeta_{sen}$  increases from 10% to 90%, and the probability of missing a target is less than 60%.

It can be observed from the previous discussion that, in TDSFO, the nodes stay in the sleep state over a period of time. Therefore, it is possible that a target passes by a node just when the node is in the long period of sleep state, and the performance monitoring of network worsens in this way. For this reason, a scheme named TDSFK is proposed. In the TDSFK scheme, the sensing period is dispersed throughout the whole cycle  $t_{sen}$ , as

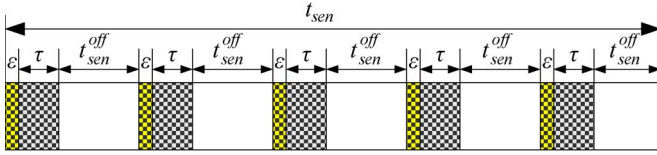


Fig. 4. TDSFK scheme (sensing frequency is  $k$ ).

shown in Fig. 4. Nodes are first converted from the sleep state to the sensing state, after the sensing time  $\tau$ , and then returned back to the sleep state. They run in circles similar to this, until the sensing cycle is complete. In this way, the sensing frequency of nodes is  $k$ , which avoids the shortage of long sleep time in a period. Hence, the target is difficult to be undetected. Fig. 3 shows the performance of TDSFK. It is thus clear that, under the same power consumption, the moving distance of target is almost only  $1/k$  of the original in TDSFK, which greatly enhances the network monitoring performance.

### B. Calculation of Sensing Frequency $k$

First, the calculation method of the sensing frequency  $k$  is presented here when adopting the TDSFK scheme instead of TDSFO, and the energy consumption of nodes remains unchanged. As in the TDSFO scheme, the state transition is one time, and in the TDSFK scheme, it is  $k$  times, and each time it needs to consume energy, its energy consumption for state transition is higher than that of TDSFO scheme. Therefore, in TDSFO scheme, when the nodes are in the sensing state, with sensing frequency  $k_1$  and sensing slot number  $\tau$ , and converted into TDSFK scheme, if the sensing frequency is  $k_2$ , then there is  $k_1 \leq k_2$ . The calculation method of  $k_2$  is given in the following.

*Theorem 1:* Assuming that the TDSFO scheme changes state only once in a sensing cycle  $t_{\text{sen}}$ , the sensing time can be divided into  $k_1$  blocks (sensing frequency is actually 1). When keeping the same total energy consumption, the greatest sensing frequency of TDSFK scheme is given by

$$k_2 \leq \frac{k_1 \tau (\varepsilon_{\text{sen}} - \varepsilon_s) + \varepsilon_c t_c}{\tau (\varepsilon_{\text{sen}} - \varepsilon_s) + \varepsilon_c t_c}. \quad (8)$$

*Proof:* Equation (6) provides the calculation formula of sensing duty cycle. Set  $t_{\text{sen}}^a = k_1 \tau$ ; after optimization,  $t_{\text{sen}}^{a'} = k_2 \tau$ .

If the total energy consumption of sensing data remains unchanged, then

$$\begin{aligned} e_c^{k_1} + e_{\text{sen}}^{k_1} &= e_c^{k_2} + e_{\text{sen}}^{k_2} \Rightarrow \varepsilon_c t_c + \left[ \frac{k_1 \tau}{t_{\text{sen}}} \varepsilon_{\text{sen}} + \varepsilon_s \left( 1 - \frac{k_1 \tau}{t_{\text{sen}}} \right) \right] t_{\text{sen}} \\ &\geq k_2 \varepsilon_c t_c + \left[ \frac{k_2 \tau}{t_{\text{sen}}} \varepsilon_{\text{sen}} + \varepsilon_s \left( 1 - \frac{k_2 \tau}{t_{\text{sen}}} \right) \right] t_{\text{sen}}. \end{aligned}$$

That is,  $\varepsilon_c t_c + k_1 \tau (\varepsilon_{\text{sen}} - \varepsilon_s) \geq k_2 \varepsilon_c t_c + k_2 \tau (\varepsilon_{\text{sen}} - \varepsilon_s)$ , where  $k_2 \leq (k_1 \tau (\varepsilon_{\text{sen}} - \varepsilon_s) + \varepsilon_c t_c) / (\tau (\varepsilon_{\text{sen}} - \varepsilon_s) + \varepsilon_c t_c)$ . ■

Fig. 5 shows the maximum  $k_2$  corresponding to  $k_1$  when the initial sensing frequency is 1. It is shown in the figure that  $k_2$  increased with the increase in  $k_1$ . When taking different  $\tau$ , the

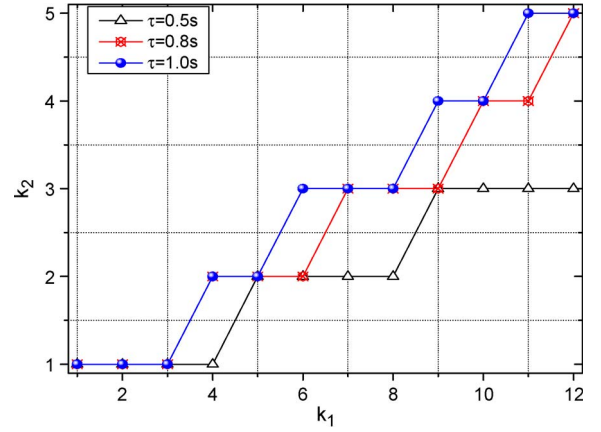


Fig. 5. Corresponding  $k_2$  when the initial sensing frequency is 1.

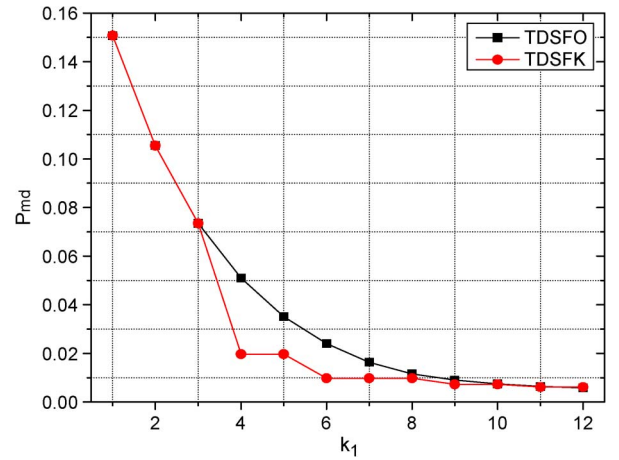


Fig. 6. Corresponding maximum  $P_{\text{md}}$  when the initial sensing frequency is 1

growth of  $k_2$  is also different. It follows that the relationship between  $k_1$ ,  $k_2$ , and  $\tau$  in (8) is correct.

### C. Performance Analysis of TDSFK Scheme

When the sensing frequency increases to  $k_2$ , the time that the sensor is in the sleeping state declines with the increase in the sensing duty cycle. The time of monitoring lengthens, and the probability of missed target detection becomes less. As Fig. 6 shows, the TDSFK scheme improves the performance of  $P_{\text{md}}$  after the frequency is dispersed. When the frequency is divided into four, the performance is improved the most.

*Theorem 2:* In the TDSFK scheme, the probability of missed target detection of nodes with sensing frequency  $k_2$  is expressed as follows:

$$P_{\text{md}}(k_2) \geq \left\{ 1 - \left[ \frac{k_2 \tau}{t_{\text{sen}}} + \left( 1 - \frac{k_2 \tau}{t_{\text{sen}}} \right) P_{\partial}(k_2) \right] \frac{r_s}{R} \right\}^N \quad (9)$$

where

$$P_{\partial}(k_2) = \begin{cases} \frac{4r_s}{\pi \eta(k_2) v}, & \text{if } \frac{2r_s}{v} < \eta(k_2) \\ \frac{4r_s - 2\sqrt{4r_s^2 - \eta(k_2)^2 v^2}}{\pi \eta(k_2) v} \\ \quad + 1 - \frac{2a \sin\left(\frac{\eta(k_2)v}{2r_s}\right)}{\pi}, & \text{else} \end{cases}$$

where  $\eta(k_2) = t_{\text{sen}}/k_2 - \tau - t_c$

*Proof:* According to [2, Th. 8], the probability of missing a target within a circular region can be expressed as

$$P_{\text{md}} \geq \left\{ 1 - [\zeta_{\text{sen}} + (1 - \zeta_{\text{sen}})P(\varepsilon_1)] \frac{r_s}{R} \right\}^N$$

If  $2r_s/v > c$

$$P\{\varepsilon_1\} = \frac{4r_s - 2\sqrt{4r_s^2 - c^2v^2}}{\pi cv} + 1 - \frac{2a \sin\left(\frac{cv}{2r_s}\right)}{\pi}$$

$$\text{else if } 2r_s/v < c, \quad P\{\varepsilon_1\} = \frac{4r_s}{\pi cv}.$$

Among them,  $r_s$  is the sensing radius of each node,  $R$  is the radius of the whole monitoring area,  $c = (1 - \zeta_{\text{sen}})t_{\text{sen}}$ .

Due to the fact that  $\zeta_{\text{sen}} = k\tau/t_{\text{sen}}$  and  $\zeta_{\text{sen}}$  varies with the change of  $k$ , therefore, let  $\eta(k_1)$  and  $\eta(k_2)$  substitute for  $c$  in the previous formula; when sensing frequency is 1, we have  $\eta(k_1) = t_{\text{sen}} - (k_1\tau + t_c)$ . In the TDSFK scheme, due to the increase in frequency, the times of state transition increases from 1 to  $k_2$ ; hence,  $\eta(k_2) = t_{\text{sen}}/k_2 - \tau - t_c$ . ■

*Theorem 3:* In TDSFK scheme proposed in this paper, the delay for detection of nodes with sensing frequency  $k_2$  is presented as (10), shown at the bottom of the page.

*Proof:* According to [2, Th. 9], if

$$\begin{aligned} \frac{L}{v} > \eta(\zeta_{\text{sen}}^x), \quad P\{\varepsilon_{\text{SoT}}, \bar{\varepsilon}_{\text{det}}\} = 0, \quad D_{\text{det}}(\zeta_{\text{sen}}^x) \\ &= E(Q)/v = \frac{(2\bar{q}_{\text{max}}r_s - \pi R^2)^{N+1}}{2\pi^N R^{2N} r_s (N+1)v} \\ \text{else if } \frac{L}{v} \leq \eta(\zeta_{\text{sen}}^x), \quad D_{\text{det}}(\zeta_{\text{sen}}^x) &= E(Q)/v \\ &= \frac{\int_0^{\bar{q}_{\text{max}}} \sum_{i=0}^N \left(1 - \frac{2qr_s}{\pi R^2}\right)^{N-i} \left(\frac{2qr_s^2}{\pi R^3} (1 - \zeta_{\text{sen}}^x) (1 + P_{\partial}(\zeta_{\text{sen}}^x))\right)^i dq}{v}. \end{aligned}$$

In the TDSFK scheme, the frequency is  $k_2$ . Replace  $\zeta_{\text{sen}}^x$  in the previous formula with  $\zeta_{\text{sen}} = k_2\tau/t_{\text{sen}}$ , and other values remain unchanged. Now, (10) is proved. ■

From (10), we can observe that the more the divided frequency, the more times the node will sense. It is easier to be detected after the target enters the network; hence, the delay will be smaller. Fig. 7 shows that the performance is improved after the frequency is divided into several fragments. In addition, when the frequency is 6, the performance improved the most.

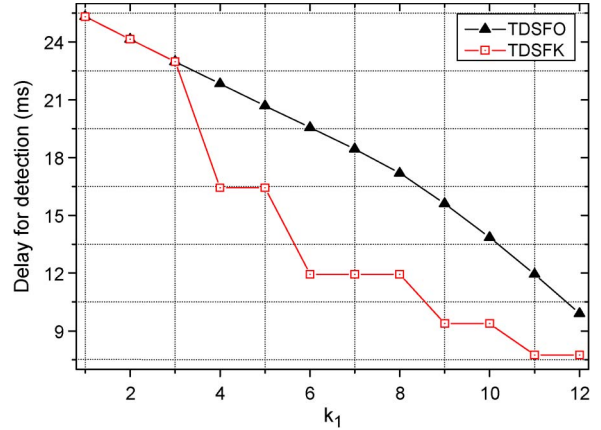


Fig. 7. Corresponding maximum  $D_{\text{det}}$  when the initial sensing frequency is  $k_1$ .

## V. TDASF SCHEME

### A. Presentation of Questions

As aforementioned, we have proposed the TDSFK scheme. The uniform dispersion of sensing time slot in the sensing cycle can improve the monitoring quality of the network. However, according to our findings, the monitoring quality of the network can be further optimized. Therefore, the TDASF scheme is presented here. Its main idea is presented as follows: the “many to one” model is applied in WSNs to collect data, and then, all the data are finally sent to the sink. In this way, a region (i.e., hotspots) around the sink is formed, and its energy consumption is higher than other regions, which leads to an early death of the network. This phenomenon is called the “energy hole.” Many studies indicate that, when the sensor network dies in advance because of the “energy hole,” there still remains as much as 90% energy. Thus, the TDASF scheme makes full use of the remaining energy by increasing the sensing frequency energy of nodes in the nonhotspot region. Generally speaking, the farther the node is away from the sink, the more its residual energy, the higher sensing frequency is needed, and vice versa. Hence, this kind of scheme using different sensing frequency in different areas is called the TDASF scheme.

### B. Calculation of Adjustable Sensing Frequency

The main idea of the TDASF scheme is to improve the sensing frequency of nodes far away from the sink by using their residual energy, which can improve the quality of monitoring. Therefore, we first calculate the energy consumption of the nodes in different regions at different distances from the sink. The information can help to calculate the remaining energy consumption of nodes in different places, and then, the sensing frequency of different nodes can also be computed.

$$D_{\text{det}}(k_2) = \begin{cases} \frac{(2\bar{q}_{\text{max}}r_s - \pi R^2)^{N+1}}{2\pi^N R^{2N} r_s (N+1)v}, & \text{if } \frac{L}{v} > \eta(k_2) \\ \frac{\int_0^{\bar{q}_{\text{max}}} \sum_{i=0}^N \left(1 - \frac{2qr_s}{\pi R^2}\right)^{N-i} \left(\frac{2qr_s^2}{\pi R^3} \left(\frac{1}{k_2} - \frac{\tau}{t_{\text{sen}}}\right) (1 + P_{\partial}(k_2))\right)^i dq}{v}, & \text{else.} \end{cases} \quad (10)$$

The following Theorem 4 gives the energy situation of nodes at different distances from the sink.

*Theorem 4:* At the region  $x$  meters away from the sink, the energy consumption of the nodes is as follows:

$$\omega_{\text{tot}}^x = \omega_{\text{sen}}^x + \omega_{\text{LPL}}^x + \omega_R^x \delta_r^x + \omega_T^x \delta_t^x + w_c^x. \quad (11)$$

*Proof:* With the different distances to the sink, the data amount of node varies from area to area; hotspot nodes have to receive and forward more data packets.

$\omega_{\text{tot}}^x$  denotes the total power consumed by sensing and communication operations of the nodes at  $x$  meters away from the sink in a communication cycle  $t_{\text{com}}$ . According to the description of the X-MAC protocol in [6], there are four possible states in the energy consumption  $\omega_{\text{tot}}^x$ : 1) transmission, 2) reception, 3) sleep, and 4) LPL.  $\omega_{\text{sen}}^x$  denotes the power consumption for sensing in an activity duration  $t_{\text{sen}}$ .  $\omega_{\text{LPL}}^x$  is the required power of the LPL operations. Suppose that the node at  $x$  meters apart from the sink has  $\delta_t^x$  packets to be transmitted in a communication cycle  $t_{\text{com}}$  and  $\delta_r^x$  packets to be received.  $\omega_R^x$  is the power used for receiving a packet.  $\omega_T^x$  is the power for transmitting an alert packet.  $w_c^x$  is the power consumed for state transition. Summing up the aforementioned,  $\omega_{\text{tot}}^x$  can be computed by (11). ■

*Theorem 5:* Supposing that all the residual energy is used to increase the sensing frequency, then the sensing frequency of the nodes at the smallest distance is denoted by  $k^{x_{\text{min}}}$ , those at  $x$  meters away from the sink is denoted by  $k^x$ , and the relationship between  $k^{x_{\text{min}}}$  and  $k^x$  can be expressed as (12), shown at the bottom of the page.

*Proof:* The largest energy consumption comes from the nodes nearest to the sink node. From Theorem 4, we can arrive at  $x = x_{\text{min}}$ , when its energy consumption is given by

$$\begin{aligned} e_{\text{tot}}^{x_{\text{min}}} &= e_c^{x_{\text{min}}} + e_{\text{sen}}^{x_{\text{min}}} + e_{\text{LPL}}^{x_{\text{min}}} + e_T^{x_{\text{min}}} + e_R^{x_{\text{min}}} \text{ where} \\ e_c^{x_{\text{min}}} &= k^{x_{\text{min}}} \varepsilon_c t_c \quad e_{\text{sen}}^{x_{\text{min}}} = \varepsilon_{\text{sen}} k^{x_{\text{min}}} \tau + \varepsilon_s (t_{\text{sen}} - k^{x_{\text{min}}} \tau) \\ e_{\text{LPL}}^{x_{\text{min}}} &= [\varepsilon_r \varsigma_{\text{com}} + \varepsilon_s (1 - \varsigma_{\text{com}}) - \tau_t^{x_{\text{min}}} - \tau_r^{x_{\text{min}}}] t_{\text{com}} \\ e_T^{x_{\text{min}}} &= \omega_T \delta_T^{x_{\text{min}}} \quad e_R^{x_{\text{min}}} = \omega_R \delta_R^{x_{\text{min}}}. \end{aligned}$$

Suppose that the nodes nearest to the sink and those at  $x$  meters away from the sink have equal energy consumption; hence, there is  $e_{\text{tot}}^{x_{\text{min}}} = e_{\text{tot}}^x$ , which is given by the equation shown at the bottom of the page. ■

$$k^x = k^{x_{\text{min}}} - \frac{(\tau_t^{x_{\text{min}}} - \tau_t^x + \tau_r^{x_{\text{min}}} - \tau_r^x) t_{\text{com}} + \omega_T (\delta_t^x - \delta_t^{x_{\text{min}}}) + \omega_R (\delta_r^x - \delta_r^{x_{\text{min}}})}{(\varepsilon_{\text{sen}} - \varepsilon_s) \tau + \varepsilon_s t_c}. \quad (12)$$

$$\begin{aligned} e_{\text{sen}}^{x_{\text{min}}} - e_{\text{sen}}^x + e_c^{x_{\text{min}}} - e_c^x &= e_{\text{LPL}}^x + e_T^x + e_R^x - (e_{\text{LPL}}^{x_{\text{min}}} + e_T^{x_{\text{min}}} + e_R^{x_{\text{min}}}) \\ \Rightarrow (\varsigma_{\text{sen}}^{x_{\text{min}}} - \varsigma_{\text{sen}}^x) (\varepsilon_{\text{sen}} - \varepsilon_s) t_{\text{sen}} + (k^{x_{\text{min}}} - k^x) \varepsilon_c t_c &= (\tau_t^{x_{\text{min}}} - \tau_t^x + \tau_r^{x_{\text{min}}} - \tau_r^x) t_{\text{com}} \\ &+ \omega_T (\delta_t^x - \delta_t^{x_{\text{min}}}) + \omega_R (\delta_r^x - \delta_r^{x_{\text{min}}}) \\ \Rightarrow k^{x_{\text{min}}} - k^x &= \frac{(\tau_t^{x_{\text{min}}} - \tau_t^x + \tau_r^{x_{\text{min}}} - \tau_r^x) t_{\text{com}} + \omega_T (\delta_t^x - \delta_t^{x_{\text{min}}}) + \omega_R (\delta_r^x - \delta_r^{x_{\text{min}}})}{(\varepsilon_{\text{sen}} - \varepsilon_s) \tau + \varepsilon_c t_c}. \end{aligned}$$

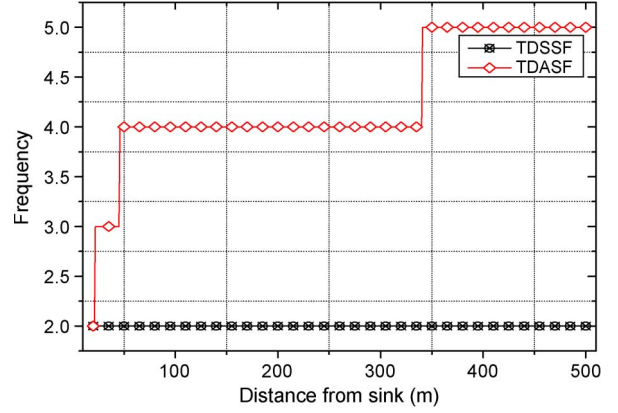


Fig. 8. Sensing frequency in different distances from the sink.

Fig. 8 shows the variation of sensing frequency in different areas in the network. It adopts the TDASF scheme, and the sensing frequency of the hotspot region is 2. Here, it is shown that, in Fig. 8, the sensing frequency that the TDASF scheme adopts in most of the region in the network is more than two times that of TDSSF. It means that the TDASF scheme can improve the monitoring quality of the network significantly.

### C. Performance Analysis

#### 1) Probability of Missed Target Detection:

##### a) Single Target Detection

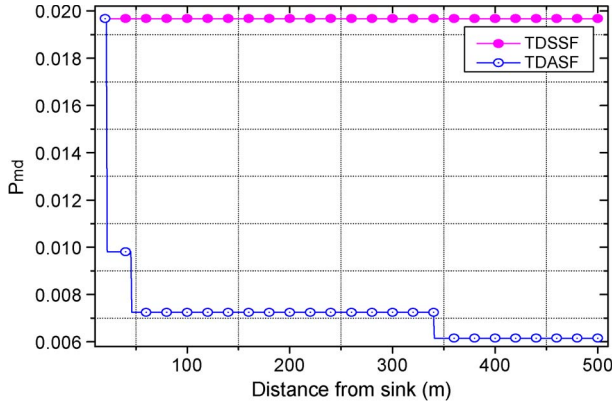
*Theorem 6:* In the TDASF scheme, the probability of missing target detection of the nodes at  $x$  meters away from the sink is expressed as follows:

$$P_{\text{md}}(k^x) \geq \left\{ 1 - \left[ \frac{k^x \tau}{t_{\text{sen}}} + \left( 1 - \frac{k^x \tau}{t_{\text{sen}}} \right) P_{\partial}(k^x) \right] \frac{r_s}{R} \right\}^N \quad (13)$$

where

$$P_{\partial}(k^x) = \begin{cases} \frac{4r_s}{\pi \eta(k^x) v}, & \text{if } \frac{2r_s}{v} < \eta(k^x) \\ \frac{4r_s - 2\sqrt{4r_s^2 - \eta(k^x)^2 v^2}}{\pi \eta(k^x) v} \\ \quad + 1 - \frac{2a \sin\left(\frac{\eta(k^x) v}{2r_s}\right)}{\pi}, & \text{else} \end{cases}$$

where  $\eta(k^x) = t_{\text{sen}}/k^x - \tau - t_c$ .


 Fig. 9.  $P_{md}$  at different distances from the sink.

*Proof:* In the network, the nodes near the sink have a larger load than those far from the sink. In order to use the residual energy of the external nodes in the network effectively, we define that the sensing frequency  $k$  of nodes increases with their distance to the sink. Therefore, the probability of target detection  $P_{md}(k^x)$  becomes a related function with  $x$ . The rest proof is the same as Theorem 2. ■

*Theorem 7:* In this paper, the weighted probability of missing target detection of the whole network is expressed as follows:

$$P_{md}^w \geq \int_0^R \int_0^{2\pi} P_{md}(k^x) \cdot x \cdot dx \cdot d\theta. \quad (14)$$

*Proof:* Let  $k^x$  be the sensing frequency of the nodes at  $x$  meters away from the sink.  $k^x$  varies with different  $x$ . Therefore, if only the weighted average of  $P_{md}(k^x)$  is calculated, then the probability of missed target detection of the whole network can be obtained.

In the place whose distance from the network center is  $x | x \in \{0, \dots, R\}$ , we take a fraction of fan-shaped ring  $\phi$  with an angle  $d\theta$  and a width of  $dx$ . The area of this region is  $x \cdot dx \cdot d\theta$ . The probability of missed target detection of the entire network can be expressed as  $x \cdot dx \cdot d\theta \cdot P_{md}(k^x)$ .

Equation (12) shows the probability of missed target detection at  $x$  meters away from the sink. Integral to the entire region, the weighted probability of missed target detection can be obtained as

$$P_{md}^w \geq \int_0^R \int_0^{2\pi} P_{md}(k^x) \cdot x \cdot dx \cdot d\theta.$$

According to Theorem 7, Fig. 9 shows the probability of missed target detection at  $x$  meters away from the sink. With the increase in distance,  $P_{md}$  of TDASF is getting to less and less, while the other line keeps horizontal. It is obvious that the TDASF scheme can significantly decrease  $P_{md}$  of external nodes.

*b) Multitarget detection:* Similar to that in [2], the probability of missed target detection of the node at  $x$  meters away from the sink is denoted by  $P_{md}(k^x)$ . Hence, the probability

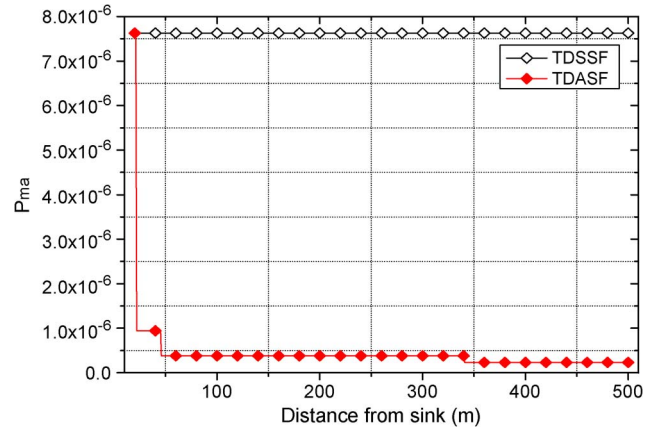
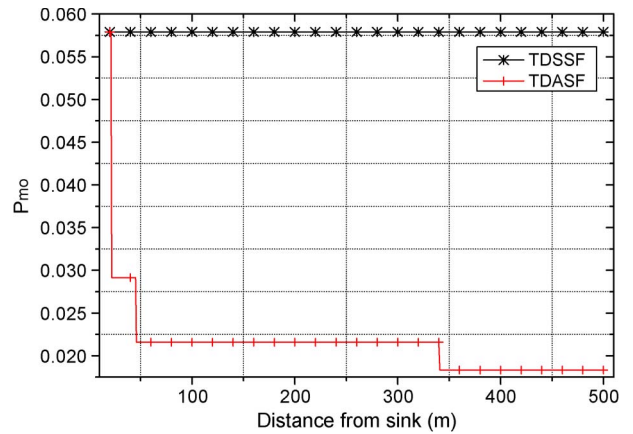
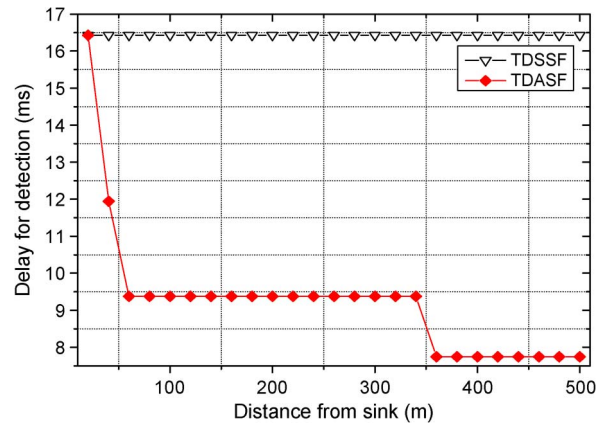

 Fig. 10. Probability of missed multiple-target detection ( $P_{ma}$ )

 Fig. 11. Probability of missed multiple-target detection ( $P_{mo}$ ).


Fig. 12. Detection delays at different distances from the sink.

of missing all and at least one out of  $N_T$  incoming targets are given respectively by

$$P_{ma}(k^x) = (P_{md}(k^x))^{N_T}$$

$$P_{mo}(k^x) = 1 - (1 - P_{md}(k^x))^{N_T}.$$

Figs. 10 and 11 give the probability of missing all and at least one out of  $N_T$  incoming targets under the TDASF and TDSSF strategies, respectively. In the figures, it can be observed that  $P_{ma}$  and  $P_{mo}$  of the TDASF scheme are markedly less than those of the TDSSF scheme.

*Theorem 8:* In TDASF, the probability of missing all incoming targets and the probability of missing at least one out of the incoming targets of the entire network are expressed as follows:

$$P_{\text{ma}}^w = \int_0^R \int_0^{2\pi} P_{\text{ma}}(k^x) \cdot x \cdot dx \cdot d\theta$$

$$P_{\text{mo}}^w = \int_0^R \int_0^{2\pi} P_{\text{mo}}(k^x) \cdot x \cdot dx \cdot d\theta. \quad (15)$$

*Proof:* In the place whose distance from the network center is  $x|x \in \{0, \dots, R\}$ , we take a fraction of fan-shaped ring  $\phi$  with an angle  $d\theta$  and a width of  $dx$ . The area of this region is  $x dx d\theta$ . The probability of missed target detection of the network can be expressed as  $x \cdot dx \cdot d\theta \cdot P_{\text{ma}}(k^x)$  and  $x \cdot dx \cdot d\theta \cdot P_{\text{mo}}(k^x)$ .

Integral to the entire region, the weighted probabilities of missed target detection are expressed as follows:

$$P_{\text{ma}}^w = \int_0^R \int_0^{2\pi} P_{\text{ma}}(k^x) \cdot x \cdot dx \cdot d\theta$$

$$P_{\text{mo}}^w = \int_0^R \int_0^{2\pi} P_{\text{mo}}(k^x) \cdot x \cdot dx \cdot d\theta.$$

## 2) Delay for Detection

*Theorem 9:* Based on the proposed weighted approach, the delay for detection at  $x$  meters away from the sink can be calculated as (16), shown at the bottom of the page.

*Proof:* In the network, the nodes near the sink have a larger load than those far from the sink. In order to use the residual energy of the external nodes in the network effectively, we define that the sensing frequency  $k$  of nodes increases with their distance to the sink. Therefore, the probability of target detection  $D_{\text{det}}(k^x)$  becomes a related function with  $x$ . The rest proof is the same as Theorem 3. ■

According to Theorem 9, Fig. 12 shows the delay for detection at  $x$  meters away from the sink. With the increase in distance,  $D_{\text{det}}$  of TDASF is getting to less and less, while the other line keeps horizontal. It is obvious that the TDASF scheme can significantly decrease  $D_{\text{det}}$  of the external nodes.

*Theorem 10:* The delay for detection of the entire network in this paper can be obtained as

$$D_{\text{det}}^w = \begin{cases} D_{\text{det}}(k^x), & \text{if } \frac{L}{v} > \eta(k^x) \\ \int_0^R \int_0^{2\pi} D_{\text{det}}(k^x) \cdot x \cdot dx \cdot d\theta, & \text{else.} \end{cases} \quad (17)$$

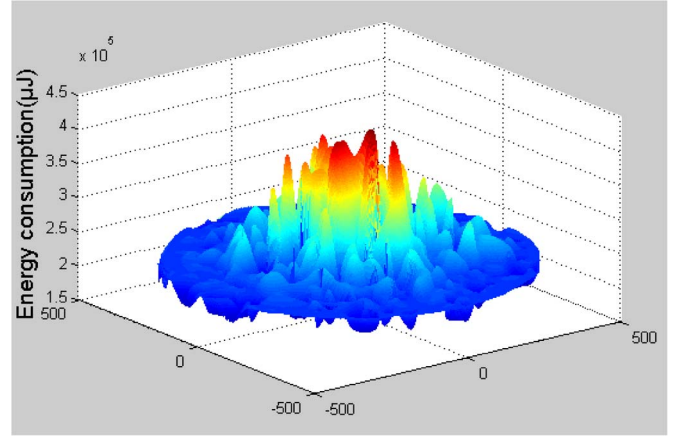


Fig. 13. Energy consumption of TDSFO scheme (lifetime = 9 rounds).

*Proof:* If  $L/v > \eta(k^x)$ ,  $D_{\text{det}}(k^x) = (2\bar{q}_{\text{max}}r_s - \pi R^2)^{N+1} / 2\pi^N R^{2N} r_s (N+1)v$ . This formula has nothing to do with  $x$ ; hence, the expression is constant.

Else if  $L/v < \eta(k^x)$ , we take the position whose distance from the network center is  $x|x \in \{0, \dots, R\}$  and then a fraction of fan-shaped ring  $\phi$  with an angle  $d\theta$  and a width of  $dx$ . The area of this region is  $x dx d\theta$ . The probability of missed target detection can be given by  $D_{\text{det}}(k^x) \cdot x \cdot dx \cdot d\theta$ .

Integral to the entire region, the weighted delay for detection  $D_{\text{det}}^w = \int_0^R \int_0^{2\pi} D_{\text{det}}(k^x) \cdot x \cdot dx \cdot d\theta$ . ■

## 3) Network Lifetime

*Theorem 11:* According to the TDASF scheme, when the sensing frequency of the hotspot is  $k^{x_{\text{min}}}$ , the lifetime of the network can be calculated as

$$\ell = \frac{E_{\text{init}}}{e_{\text{sen}}^{x_{\text{min}}} + e_{\text{LPL}}^{x_{\text{min}}} + e_T^{x_{\text{min}}} + e_R^{x_{\text{min}}} + e_c^{x_{\text{min}}}} \quad (18)$$

where  $e_{\text{sen}}^{x_{\text{min}}} = \varepsilon_{\text{sen}} k^{x_{\text{min}}} \tau + \varepsilon_s (t_{\text{sen}} - k^{x_{\text{min}}} \tau)$ ,  $e_{\text{LPL}}^{x_{\text{min}}} = [\varepsilon_r \varsigma_{\text{com}} + \varepsilon_s (1 - \varsigma_{\text{com}}) - \tau_t^{x_{\text{min}}} - \tau_r^{x_{\text{min}}}] t_{\text{com}}$ ,  $e_T^{x_{\text{min}}} = \omega_T \delta_T^{x_{\text{min}}}$ ,  $e_R^{x_{\text{min}}} = \omega_R \delta_R^{x_{\text{min}}}$ , and  $e_c^{x_{\text{min}}} = k^{x_{\text{min}}} \varepsilon_c t_c$ .

*Proof:* In TDASF, the calculation of the energy consumption is based on the maximum consumption of the hotspot nodes. The nodes nearest to the sink consume the most energy. Equation (11) shows the power consumed in a state cycle. Network lifetime means the maximum energy consumption, i.e., the initial energy  $E_{\text{init}}$  divided by the average energy consumption taking the state cycle as a unit. ■

## VI. EXPERIMENTAL RESULT

OMNET++ is used for experimental verification [20]. If not specified, the network parameters are set to  $R = 500$  m,

$$D_{\text{det}}(k^x) = \begin{cases} \frac{(2\bar{q}_{\text{max}}r_s - \pi R^2)^{N+1}}{2\pi^N R^{2N} r_s (N+1)v}, & \text{if } \frac{L}{v} > \eta(k^x) \\ \frac{\int_0^{\bar{q}_{\text{max}}} \sum_{i=0}^N (1 - \frac{2qr_s}{\pi R^2})^{N-i} \left( \frac{2qr_s^2}{\pi R^3} \left( \frac{1}{k^x} - \frac{\tau}{t_{\text{sen}}} \right) (1 + P_{\partial}(k^x)) \right)^i dq}{v}, & \text{else} \end{cases} \quad (16)$$

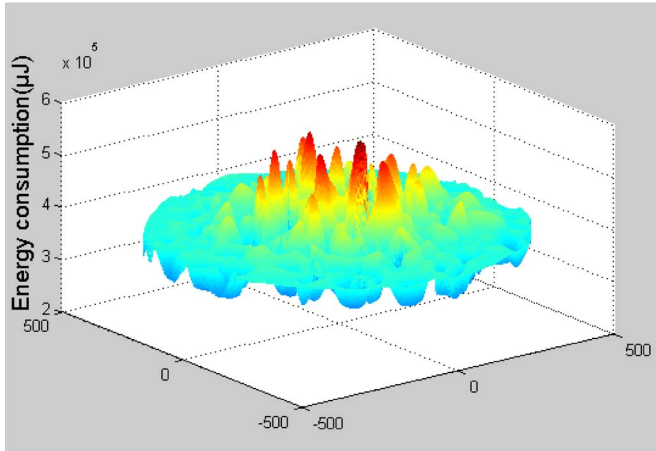


Fig. 14. Energy consumption of TDSFK scheme (lifetime = 9 rounds).

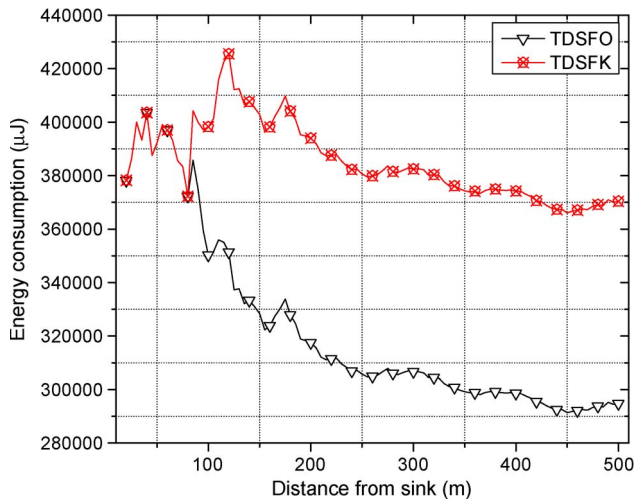


Fig. 15. Total energy consumption.

$r = 80$  m, and the number of nodes is 1000. Other experimental parameters and symbols are presented in Table I.

### A. Energy Consumption

Figs. 13 and 14 show the energy consumption of the network under different schemes. As shown in the figures, the energy consumption of the TDSFK is basically balanced when the lifetime is not lower than that of the TDSFO. This represents that the new scheme has efficiently balanced the energy of the whole network.

Fig. 15 is the total energy consumption of all the operations, which includes data communication, sleep state, energy for conversion, and LPL operations. It seems obvious that, in TDSFK, the energy line of the network is much more balanced than below. This fully testifies to the necessity of the new scheme.

### B. Network Lifetime

This section mainly compares the lifetime of TDASF and TDSSF schemes under the same monitoring performance requirements. The following comparative results make use of

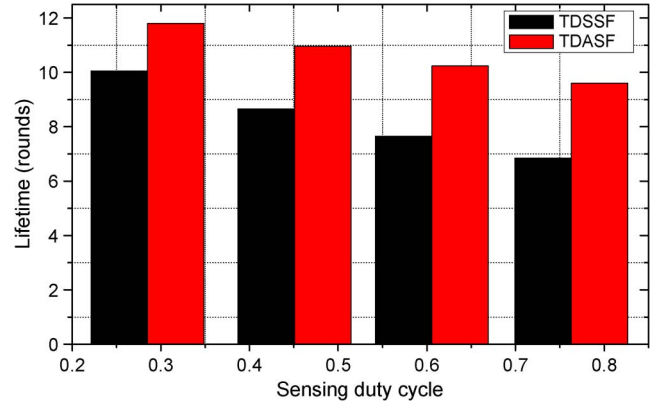


Fig. 16. Comparative lifetime of different schemes under the same weighted sensing duty cycles.

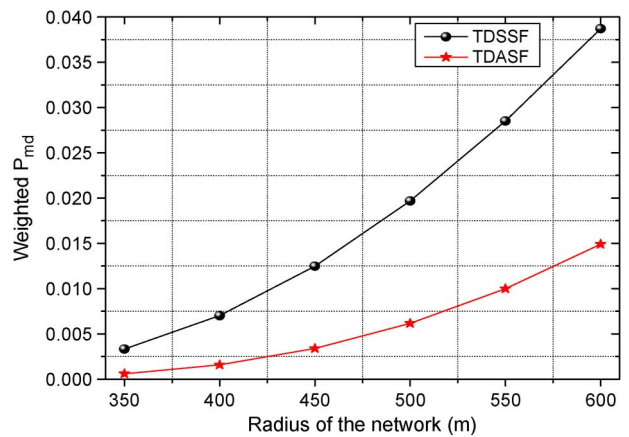


Fig. 17. Weighted probability of missed target detection under different network radius  $R$ .

the same weighted performance in order to ensure fairness. In the next place, the following experiment is the monitoring performances of TDASF compared to TDSSF when they share the same lifetime.

Fig. 16 shows the comparative lifetime in different schemes when adopting the same weighted sensing duty cycles. TDASF can improve the network lifetime by 17.4%–40.1% in the figure.

### C. Probability of Missed Target Detection

Fig. 17 shows the weighted probability of missed target under different network radius  $R$ . In this figure, the line in red that denoted the value of the weighted probability of missed target is much less than the other one. In addition, with the increasing of network radius, the growth is slower. The weighted probability of missed target detection of TDSSF is 2.6 to 4.8 times the value of TDASF. This illustrates that TDASF is more suitable for the large-scale network.

As shown in Figs. 18 and 19, the weighted probability of missing all and at least one out of the  $N_T$  incoming targets are given under the different network radius  $R$ , respectively. This shows that  $P_{ma}^w$  and  $P_{mo}^w$  of TDASF are much less than those of TDSSF.

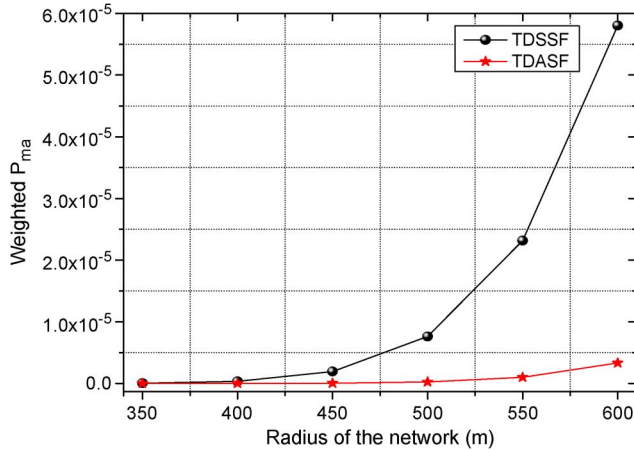


Fig. 18. Weighted  $P_{ma}$  under different network radius  $R$ .

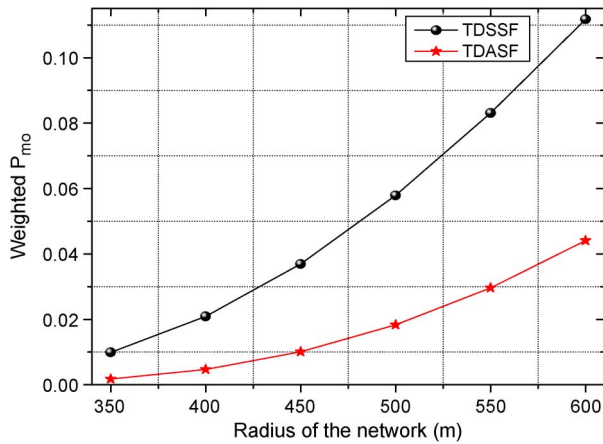


Fig. 19. Weighted  $P_{mo}$  under different network radius  $R$ .

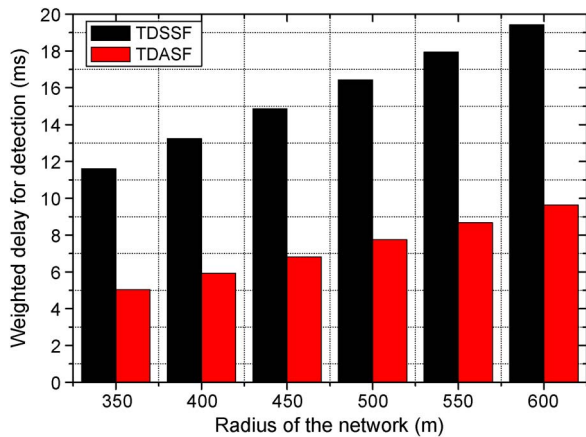


Fig. 20. Weighted delays for detection.

#### D. Delay for Detection

According to Theorem 10, the comparison of weighted delay for detection between TDSSF and TDASF can be obtained. It is shown in Fig. 20 that, under the same  $\zeta_{sen}^{x_{min}}$  and different network radius, the weighted detection delays were reduced by 101.6%–130%. This illustrates the effectiveness of the TDASF strategy.

## VII. CONCLUSION

In this paper, we have proposed an intelligent adjustable sensing frequency for mobile target detection based on the monitor quality optimization. Two schemes named TDSFK and TDASF are proposed. In the first scheme, the unequal sensing frequency in different regions is used to improve the monitor quality by taking the advantages of the residual energy throughout the network. The second scheme provides the method for the calculation of proper frequency value. The evaluation of the performances of the proposed schemes was made with three parameters: probability of missed target, delay, and lifetime. Computer simulation results show that the TDASF scheme can improve the network lifetime by more than 17.4% and can reduce the weighted detection delay by more than 101.6%. The algorithm proposed in this paper is for the static sink WSNs, which is not suitable for mobile sink networks. Therefore, our further work is to explore the optimization problem of target detection in mobile sink network.

## REFERENCES

- [1] J. Gubbi, R. Buyya, S. Marusic, and M. Palaniswami, "Internet of Things (IoT): A vision, architectural elements, and future directions," *Future Gen. Comput. Syst.*, vol. 29, no. 7, pp. 1645–1660, Sep. 2013.
- [2] P. Medagliani, J. Leguay, G. Ferrari, V. Gay, and M. Lopez-Ramos, "Energy-efficient mobile target detection in wireless sensor networks with random node deployment and partial coverage," *Pervasive Mobile Comput.*, vol. 8, no. 3, pp. 429–447, Jun. 2012.
- [3] D. Zhang, Z. Yang, V. Raychoudhury, Z. Chen, and J. Lloret, "An energy-efficient routing protocol using movement trend in vehicular ad-hoc networks," *Comput. J.*, vol. 56, no. 8, pp. 938–946, Aug. 2013.
- [4] Y. Mo, B. Wang, W. Liu, and L. Yang, "A sink-oriented layered clustering protocols for wireless sensor networks," *Mobile Netw. Appl.*, vol. 18, no. 5, pp. 639–650, Oct. 2013.
- [5] B. Wang, H. B. Lim, and D. Ma, "A coverage-aware clustering protocol for wireless sensor networks," *Comput. Netw.*, vol. 56, no. 5, pp. 1599–1611, Mar. 2012.
- [6] B. Wang, H. B. Lim, and D. Ma, "Broadcast based on layered diffusion in wireless ad hoc and sensor networks," *Wireless Commun. Mobile Comput.*, vol. 12, no. 1, pp. 99–115, Jan. 2012.
- [7] P. Medagliani, G. Ferrari, V. Gay, and J. Leguay, "Cross-layer design and analysis of WSN-based mobile target detection systems," *Ad Hoc Netw.*, vol. 11, no. 2, pp. 712–732, Mar. 2013.
- [8] C. F. Huang, Y. C. Tseng, and L. C. Lo, "The coverage problem in three-dimensional wireless sensor networks," *J. Intercon. Netw.*, vol. 8, no. 3, pp. 209–227, Sep. 2007.
- [9] S. Megerian, F. Koushanfar, M. Potkonjak, and M. B. Srivastava, "Worst and best-case coverage in sensor networks," *IEEE Trans. Mobile Comput.*, vol. 4, no. 1, pp. 84–92, Jan./Feb. 2005.
- [10] B. Liu and D. Towsley, "A study of the coverage of large-scale sensor networks," in *Proc. IEEE MASS*, 2004, pp. 475–483.
- [11] R. R. Rout and S. K. Ghosh, "Enhancement of lifetime using duty cycle and network coding in wireless sensor networks," *IEEE Trans. Wireless Commun.*, vol. 12, no. 2, pp. 656–667, Feb. 2013.
- [12] K. Han, J. Luo, Y. Liu, and A. Vasilakos, "Algorithm design for data communications in duty-cycled wireless sensor networks: A survey," *IEEE Commun. Mag.*, vol. 51, no. 7, pp. 107–113, Jul. 2013.
- [13] C. C. Hsu, Y. Y. Chen, C. F. Chou, and L. L. Golubchik, "On design of collaborative mobile sensor networks for deadline-sensitive mobile target detection," *IEEE Sensors J.*, vol. 13, no. 8, pp. 2962–2972, Aug. 2013.
- [14] H. Byun and J. Yu, "Adaptive duty cycle control with queue management in wireless sensor networks," *IEEE Trans. Mobile Comput.*, vol. 12, no. 6, pp. 1214–1224, Jun. 2013.
- [15] K. Ota *et al.*, "ORACLE: Mobility control in wireless sensor and actor networks," *Comput. Commun.*, vol. 35, no. 9, pp. 1029–1037, May 2012.
- [16] T. L. Chin, P. Ramanathan, and K. K. Saluja, "Modeling detection latency with collaborative mobile sensing architecture," *IEEE Trans. Comput.*, vol. 58, no. 5, pp. 692–705, May 2009.
- [17] P. K. Sahoo, J. P. Sheu, and K. Y. Hsieh, "Target tracking and boundary node selection algorithms of wireless sensor networks for internet services," *Inf. Sci.*, vol. 230, pp. 21–38, May 2013.

[18] J. C. Chin, Y. Dong, W. K. Hon, C. Y. T. Ma, and D. K. Y. Yau, "Detection of intelligent mobile target in a mobile sensor network," *IEEE/ACM Trans. Netw.*, vol. 18, no. 1, pp. 41–52, Feb. 2010.

[19] B. D. Lee and K. H. Lim, "An energy-efficient hybrid data-gathering protocol based on the dynamic switching of reporting schemes in wireless sensor networks," *IEEE Syst. J.*, vol. 6, no. 3, pp. 378–387, Sep. 2012.

[20] OMNet++ Network Simulation Framework [EB/OL]. [Online]. Available: <http://www.omnetpp.org>

[21] A. F. Liu, Z. M. Zheng, C. Zhang, Z. G. Chen, and X. M. Shen, "Secure and energy-efficient disjoint multi-path routing for WSNs," *IEEE Trans. Veh. Technol.*, vol. 61, no. 7, pp. 3255–3265, Sep. 2012.



**Kaoru Ota** (M'12) received the M.Sc. degree from Oklahoma State University, Stillwater, OK, USA, in 2008 and the Ph.D. degree from the University of Aizu, Aizuwakamatsu, Japan, in 2012.

She is an Assistant Professor with the Muroran Institute of Technology, Muroran, Japan. Her research interests include wireless networks and ubiquitous computing.



**Anfeng Liu** received the M.Sc. and Ph.D. degrees in computer science from the Central South University, Changsha, China, in 2002 and 2005, respectively.

He is a Professor with the School of Information Science and Engineering, Central South University. His major research interest includes wireless sensor networks.

Prof. Liu is also a member (E200012141M) of the China Computer Federation.



**Minyi Guo** (SM'07) received the Ph.D. degree in computer science from the University of Tsukuba, Tsukuba, Japan.

He is currently a Zhiyuan Chair Professor and Head of the Department of Computer Science and Engineering, Shanghai Jiao Tong University, Shanghai, China.

Dr. Guo is a member of the Association for Computing Machinery and the China Computer Federation. He is an Associate Editor of *IEEE TRANSACTIONS ON PARALLEL AND DISTRIBUTED SYSTEMS* and *IEEE TRANSACTIONS ON COMPUTERS*. He was a recipient of the National Science Fund for Distinguished Young Scholars from the National Natural Science Foundation of China (NSFC) in 2007.



**Yanling Hu** received the B.Sc. degree in 2013 from the Central South University, Changsha, China, where she is currently working toward the M.S. degree in the School of Information Science and Engineering.

Her research interest includes wireless sensor networks.



**Mianxiong Dong** (M'13) received the B.S., M.S., and Ph.D. degrees from the University of Aizu, Aizuwakamatsu, Japan, all in computer science and engineering.

He is currently with the National Institute of Information and Communications Technology (NICT), Tokyo, Japan. His research interests include wireless sensor networks, vehicular ad-hoc networks, and wireless security.